# Effect of oxygen pressure on stoichiometric transfer in laser ablation of Pr3+ doped Gd2O3–Ga2O3 binary system

Jan Lancok, Michal Novotny, Lenka Volfova, Joris More-Chevalier, Antonio Pereira

JVST A
Journal of Vacuum Science & Technology A

# Effect of oxygen pressure on stoichiometric transfer in laser ablation of $Pr^{3+}$ doped $Gd_2O_3$–$Ga_2O_3$ binary system

Cite as: J. Vac. Sci. Technol. A **39**, 043403 (2021); https://doi.org/10.1116/6.0001001
Submitted: 25 February 2021 . Accepted: 20 April 2021 . Published Online: 11 May 2021

Jan Lancok, Michal Novotny, Lenka Volfova, Joris More-Chevalier, and Antonio Pereira

JVST A
Journal of Vacuum Science & Technology A

ARTICLE

avs.scitation.org/journal/jva

# Effect of oxygen pressure on stoichiometric transfer in laser ablation of $Pr^{3+}$ doped $Gd_2O_3$–$Ga_2O_3$ binary system

Cite as: J. Vac. Sci. Technol. A 39, 043403 (2021); doi: 10.1116/6.0001001
Submitted: 25 February 2021 · Accepted: 20 April 2021 ·
Published Online: 11 May 2021



Jan Lancok,[1,a)] Michal Novotny,[1] Lenka Volfova,[1,2] Joris More-Chevalier,[1] and Antonio Pereira[3]

## AFFILIATIONS

[1]Institute of Physics, Czech Academy of Sciences, Na Slovance 2, 18221 Prague, Czech Republic
[2]Faculty of Science, Charles University, Hlavova 2030/8, 12843 Praha 2, Czech Republic
[3]Univ. Lyon, Université Claude Bernard Lyon 1, CNRS, Institut Lumière Matière, UMR 5306, F-69622, Villeurbanne, France

**Note:** This paper is part of the Special Topic Collection on Gallium Oxide Materials and Devices.
[a)]**Electronic mail:** lancok@fzu.cz

## ABSTRACT

Three different compounds, cubic $Gd_2O_3$, orthorhombic $GdGaO_3$, and cubic $Gd_3Ga_5O_{12}$ doped with $Pr^{3+}$ ions were fabricated as waveguiding films by pulsed laser deposition from the same target material, $Pr^{3+}$ doped $Gd_3Ga_5O_{12}$ (Pr:GGG) single crystal. All of them were deposited at the same substrate temperature of 800 °C. The different crystalline phases obtained depend only on the ambient oxygen pressure and the substrate type (YAG or YAP single crystals). The structural and texture properties of the films were analyzed by x-ray diffraction. $Pr^{3+}$ fluorescence properties were found to be similar to those of the bulk crystals. The refractive indices and waveguiding properties of the films were determined. The fluorescence properties of $Pr^{3+}$ doping ions and the refractive index of the film are presented. The oriented crystalline Pr:$GdGaO_3$ and Pr:GGG films show waveguiding propagation with attenuation around 2.5 and 1 dB/cm, respectively.



## I. INTRODUCTION

Pulsed laser deposition (PLD) is a very powerful technique to grow crystalline complex-oxide waveguides especially because of the possibility to transfer materials from the target to the film and keeping the stoichiometry.[1–7] Nevertheless, because of some processes, such as target ablation, transportation of the ablated species from the target to the substrate during the expansion of the plasma plume, and films growth regime, occurring during thin film deposition by this technique, the composition of the films can also significantly differ from the bulk.[8] For example, the reaction of the ablated species of the plasma plume with oxygen or nitrogen ambient atmosphere during the plasma plume expansion leads to a very suitable variation of this technique, called reactive-PLD, for the fabrication of oxide and nitride thin films, respectively. Reactive-PLD has been successfully applied to fabricate thin films of oxides such as $TiO_2$,[9,10] $Y_2O_3$,[11] $Al_2O_3$,[12] ZnO,[13,14] $Ga_2O_3$,[15] and nitrides such as $CN_x$, AlN, TiN, BN, and GaN (see, for example, the review[16]). Unfortunately, in some cases, the composition of the films grown by the PLD process could be changed dramatically and unfavorably by many different mechanisms. As an example, Atanasov *et al.* reported that a strong variation of potassium gadolinium ratio, which depends on both ambient gas and pressure, occurs in films grown by laser ablation from the potassium gadolinium tungstate [$KGd(WO_4)_2$] crystal target.[17] In our previous study concerning the deposition of waveguiding Pr:$Gd_3Ga_5O_{12}$ (Pr:GGG) films from the Pr:GGG single crystalline target, a strong dependence of the Ga content in the film as a function of oxygen ambient pressure at constant substrate temperature was found. Films with [Ga]:[Gd] atomic ratio significantly different from those of the GGG single crystal target were deposited depending on the oxygen ambient pressure, due to decomposition of the crystalline target induced by excimer laser radiation.[18]

According to the phase diagram of the $Gd_2O_3$–$Ga_2O_3$ binary system,[19,20] four different crystalline materials may be obtained: orthorhombic $Gd_3GaO_6$ (PDF-01-89-6631), monoclinic $Gd_4Ga_2O_9$ (stable only above 1490 °C, PDF-00-38-0505), orthorhombic

$GdGaO_3$ (PDF 01-70-238), and cubic $Gd_3Ga_5O_{12}$ (PDF-00-13-0493). Gadolinium gallium garnet $Gd_3Ga_5O_{12}$ (GGG) crystal has been intensively studied for a long time.[21] Among others, only amorphous $GdGaO_3$ (GGO) films grown by PLD for resistive switching were reported.[22] However, orthorhombic perovskite-like $GdGaO_3$, which has the same crystalline space group [Pbnm(62)] with a = 5.32 Å, b = 5.54 Å, c = 7.61 Å as the well known $YAlO_3$ (YAP) crystal, could be a promising material for laser or scintillation applications. This gadolinium gallium perovskite crystal (GGP) was synthesized for the first time by Marezio *et al.*[23] at high pressure and high temperature from GGG crystal. It is very difficult to grow the rare-earth orthogallates ($ReGaO_3$) because in oxide compounds the $Ga^{3+}$ cations strongly prefer tetrahedral coordination. The gallium in the garnet cations occupy tetrahedral and octahedral sites, while in the perovskite structure they are all in octahedral sites. Consequently, it is difficult to obtain the perovskite phase and only a few works about the $GdGaO_3$ crystal have been presented up to now.[19,20,23–25]

$Pr^{3+}$ ion in various crystals is well known for exhibiting a very rich emission spectrum extending from the ultraviolet to the infrared region and suitable lifetimes of the excited states for short-wavelength up-conversion laser materials.[26,27] Moreover, this ion can be used as a structural probe because its fluorescence emissions from $^1D_2$ and $^3P_0$ levels are very sensitive to the crystal site symmetry.[28] $Pr^{3+}$ doped materials were produced a nondegenerate two wavelength upconversion excitation pathway of 1020 and 850 nm leading to visible light emission.[29]

In our previous work focused on the plasma characterization during the GGG crystal ablation, we found a strong dependence of the plasma properties on the partial oxygen pressure. Depending on the oxygen pressure, the ratio of emission from [Gd] and [Ga] in plasma varied from 3:5 to 1:1 and GGP crystal could be fabricated on the perovskite substrate.[30]

In this work, we present the possibility to deposit crystalline waveguiding films of not only GGG but also GGP and $Gd_2O_3$, from the same target material, namely, the GGG single crystal, by the only variation of partial oxygen ambient pressure and substrate nature. Attention is particularly focused on the optical and fluorescence properties of Pr-doped GGP crystals.

## II. EXPERIMENT

The films were fabricated by PLD using a KrF excimer laser operated at 248 nm wavelength, operating up to 550 mJ output pulse energy with a repetition rate of 20 Hz. The homogeneous central part of the laser beam was focused on employing a quartz objective to the target onto a rectangular spot of $2.5 \times 4\ mm^2$ area. The majority of samples were deposited at a constant laser energy density equal to $2\ J/cm^2$. The effect of laser energy density was examined in the range 0.5– $5\ J/cm^2$ by variation of the laser output energy. Polished GGG single crystal targets, doped with 1 at. % of $Pr^{3+}$, were obtained from Czochralski grown crystals.[31] The deposition process was carried out in a vacuum chamber (base pressure $10^{-3}$ Pa) in an oxygen atmosphere at various pressures between 0.1 and 10 Pa or in argon ambient gas at a constant pressure of 10 Pa. The substrates, one single crystalline plates with dimension $10 \times 10\ mm^2$ of cubic (100) $Y_3Al_5O_{12}$ (YAG, a = 12.01 Å, PDF 00-33-0040) and orthorhombic (010) $YAlO_3$ (YAP, a = 5.33 Å, b = 7.37 Å, c = 5.18 Å, PDF 00-33-0041) polished on one side, were positioned 45 mm away from the target and mounted on a massive resistively heated holder. Silver paste was used to obtain good thermal contact between the holder and the substrate. In this way, a constant substrate temperature ($T_S$) equal to 800 °C was kept during all depositions.

The composition of the films was investigated by Rutherford Backscattering Spectroscopy (RBS) using 1.5 MeV $He^+$ ions. The crystallinity of the grown films was characterized by conventional x-ray diffraction (XRD) using Cu Kα radiation in θ–2θ arrangement. X-ray texture analyses and ω-scan of the GGP film deposited on the YAP substrate were performed on a Seifert 4-circle diffractometer in the Schulz reflection geometry. Copper radiation emitted from the x-ray tube was monochromatized ($\lambda_{CuK\alpha} = 1.5418$ Å) and collimated using a 2D multilayer optic from Xenocs company.[32] Stereographic pole figures were measured by scanning the tilt angle χ between 0° and 90° in steps of 2° and the azimuthal angle Φ between 0° and 360° in steps of 1°. The pole figures are the projection of the diffraction intensity of a given Bragg reflection as the sample is rotated.

The accurate measurement of thickness and refractive index was performed by m-line spectroscopy, assuming a step index profile.[33] The measurements were performed at 632.8 and 543 nm wavelengths using an He-Ne laser beam coupled into the films by means of an $SrTiO_3$ prism in both TE (transverse electric) and TM (transverse magnetic) polarizations. The waveguiding properties were characterized by recording the light scattered along the propagation path of the laser beam with a CCD camera.[34]

Fluorescence spectra and decays under pulsed laser excitation were measured using an excimer (XeCl, λ = 308 nm, Lumonics)-pumped dye laser (Lumonics, Model Hyperdye 300) delivering pulses of 10 ns duration and $0.1\ cm^{-1}$ spectral width with a 10 Hz repetition rate. Coumarin 480 and 440 dyes were used for excitations in the $^3P_0$ and $^3P_2$ levels of $Pr^{3+}$ ions, respectively. The fluorescence was excited tangentially and collected perpendicularly to the film surface. The fluorescence was analyzed with a Hilger and Watts 1 m monochromator (grating of 1200 grooves/mm blazed at 500 nm), detected using an RCA 31034 cooled AsGa photomultiplier, and recorded by an Ortec photon-counting system for the spectral data and a Canberra multichannel analyzer for the decay measurements.

## III. RESULTS AND DISCUSSION

### A. Film and target composition

In our previous work concerning Pr:GGG films deposited on YAG substrates, a strong dependence of the film composition, determined by RBS, on the oxygen ambient pressure ($p_O$) was presented.[18]

Figure 1 compares the evolution of the [Ga]:[Gd] atomic ratio with oxygen partial pressure for films deposited on YAG (stars) to that of films deposited on YAP (triangle) substrates at constant $T_S$ equal to 800 °C. In this graph, the point at zero oxygen pressure represents the film grown in pure argon ambient at a pressure of 10 Pa. As can be seen from these dependencies, the composition of the films does not depend on the substrate nature (YAG or YAP) at

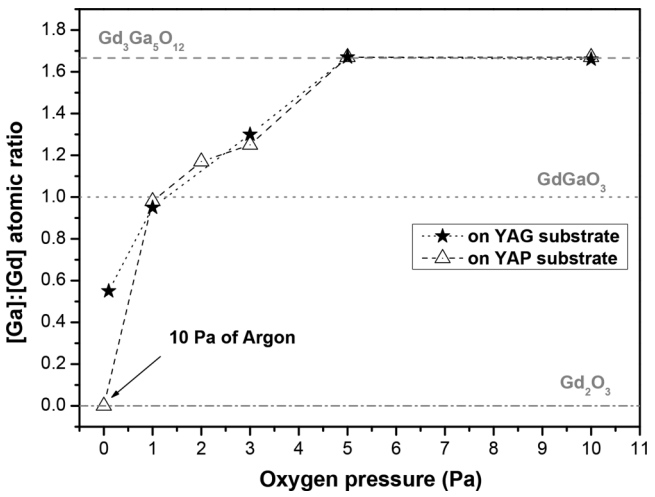


**FIG. 1.** Dependence of the [Ga]:[Gd] atomic ratio, obtained from RBS measurements, of films deposited on YAG (star) and YAP (triangle) from the Pr:GGG target at a substrate temperature equal to 800 °C as a function of pressure and substrate nature. The films deposited at 0 Pa of oxygen denote the film fabricated at 10 Pa of argon ambient.

oxygen pressures 5 and 10 Pa as is also given in Table I. As was shown in our previous work,[18] the Ga content in the films does not depend on the substrate temperature, at least in the range 700–800 °C. Considering this fact, in the present study we focused on the substrate temperature of 800 °C in respect to better crystallinity of the fabricated films. The composition of the films corresponds to that of the GGG target only for high oxygen pressure 5–10 Pa. As $p_O$ decreases, the films become strongly Ga deficient. For the film deposited on YAP substrates in argon ambient, the presence of Ga is no more detected by RBS analysis and the film composition corresponds to pure gadolinium oxide.

Spatially resolved measurements of the target composition performed by energy dispersive x ray after depositions,[18] and optical emission spectroscopy of the plasma plume[30] proved that a variation of the GGG single crystal target composition is induced by the KrF laser radiation. Decomposition of $Ga_2O_3$ to very volatile $Ga_2O$, which is promoted by low oxygen pressure,[35] and subsequent evaporation of $Ga_2O$ from the surface of the target has to be found as the main reason why the Ga content inside the film depends so strongly on the oxygen partial pressure and does not depend on the substrate nature.

The [Ga]:[Gd] ratios, as a function of oxygen pressure and substrate nature, are given in Table I, which presents also the crystalline properties as well as growth rate, thickness, and refractive index data of the films.

## B. Crystalline structure

The crystalline structure of the films deposited on (100) YAG substrates was already described in Ref. 18 and briefly recalled here. At oxygen pressure in the range 5–10 Pa, (100) oriented Pr:GGG films were deposited [Fig. 2(a)]. The films grow exclusively with (100) planes parallel to the substrate. On the contrary, at oxygen pressure lower than 1 Pa, strongly Ga deficient amorphous films were deposited even at a substrate temperature of 800 °C. In the case of the YAG substrate, no diffraction lines, which could be associated with crystalline compounds different from GGG, were observed.

The situation is different for the (010) YAP substrates, which were also used because YAP has an orthorhombic structure as most of the above-mentioned crystalline compounds containing Gd, Ga, and O. Figure 2(b) shows the XRD experimental pattern (dots) together with the modeling of the diffraction lines by Voigt functions (line) in the range of 27°–36° in 2θ, where the strongest

**TABLE I.** Dependence on oxygen pressure and substrate nature of the composition, structure, and optical properties of films deposited at substrate temperature 800 °C by ablation of a Pr:GGG target. The accuracy of the refractive indices is in the range of ±0.001.

| Oxygen pressure (Pa) | 0<br>10 Pa of Argon | 0.1 | 1 | 3 | 5 | 10 |
|---|---|---|---|---|---|---|
| *On YAP substrates* | *(110) $Gd_2O_3$* | — | *(100) $GdGaO_3$* | *GGG polycr.* | *GGG polycr.* | *GGG polycr.* |
| [Ga]:[Gd] | 0 | — | 0.98 | 1.25 | 1.60 | 1.66 |
| Refractive index at 633 nm (TE) | 1.9774 | — | $n_{TE} = 2.071$; $n_{TM} = 2.028$ | 1.960 | 1.961 | 1.963 |
| 543 nm (TE) | | | $n_{TE} = 2.122$; $n_{TM} = 2.072$ | 1.961 | 1.966 | 1.966 |
| Film growth rate (Å/pulse) | 0.928 | — | 0.725 | 0.902 | 1.149 | 1.263 |
| Film thickness (nm) | 3712 | | 2900 | 3608 | 4596 | 5052 |
| Fluorescence decay (μs) | ($^1D_2$); 57 | | ($^3P_0$); 11 | ($^3P_0$); 14 | ($^3P_0$); 17 | ($^3P_0$); 21 |
| *On YAG substrates* | — | *Amorphous* | *Amorphous* | *(100) GGG* | *(100) GGG* | *(100) GGG* |
| [Ga]:[Gd] | — | 0.55 | 0.95 | 1.32 | 1.67 | 1.66 |
| Refractive index at 633 nm (TE) | — | 1.978 | 1.972 | 1.968 | 1.964 | 1.964 |
| 543 nm (TE) | | 1.991 | 1.975 | 1.970 | 1.967 | 1.967 |
| Film growth rate (Å/pulse) | — | 0.837 | 1.103 | 1.163 | 1.183 | 1.195 |
| Film thickness (nm) | | 3375 | 4412 | 4652 | 4794 | 4845 |
| Fluorescence decay (μs) | — | ($^3P_0$); 10 | ($^3P_0$); 11 | ($^3P_0$); 21 | ($^3P_0$); 22 | ($^3P_0$); 22 |

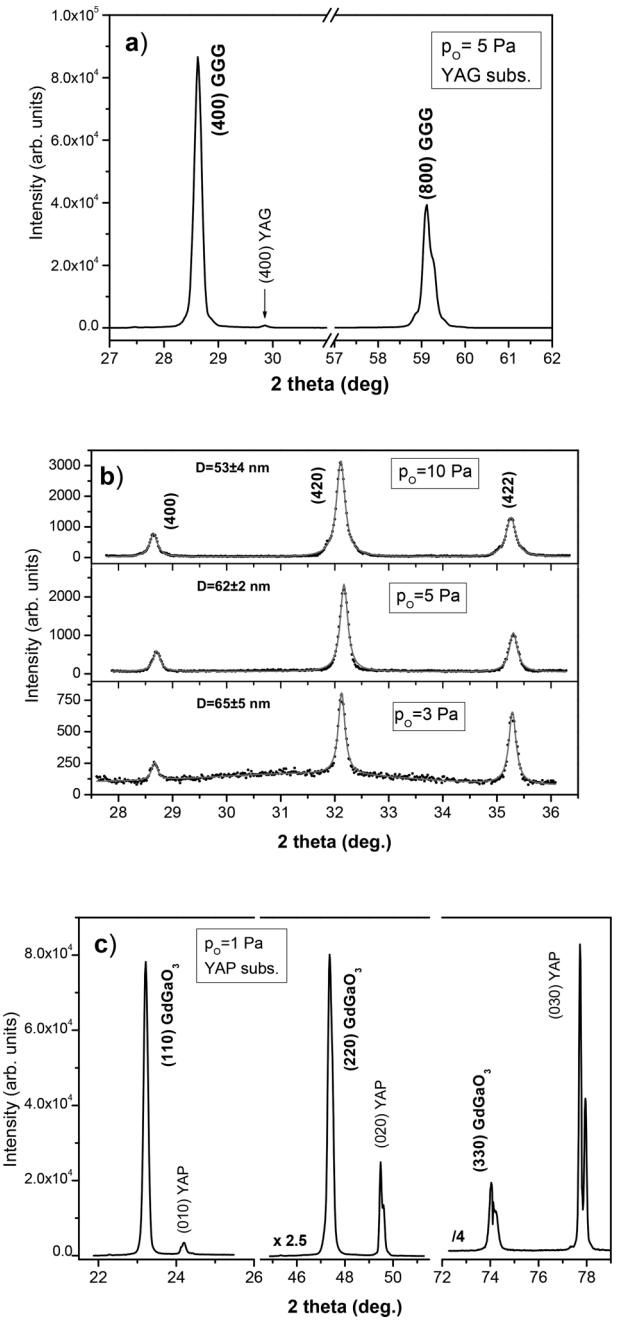


**FIG. 2.** XRD patterns of the films deposited from the Pr:GGG target at 800 °C on (a) YAG and [(b) and (c)] YAP substrates at different oxygen pressures.

diffraction peaks of GGG [(400), (420), and (422)] are located. At oxygen pressures in the range 5–10 Pa, polycrystalline GGG films with no preferential orientation were deposited because of different crystalline structures and large lattice mismatch between YAP and GGG crystals. As $p_O$ decreases to 3 Pa [Fig. 2(b)], the intensities of the diffraction peaks associated with reflections from GGG slightly decrease and a broad amorphous band located at around 31.5° appears, which indicates the presence of some additional amorphous compound in the film. Since, at these conditions, the film is significantly Ga deficient ([Ga]:[Gd] = 1.25), it probably consists of GGG crystals embedded in an amorphous matrix with a significantly lower concentration of Ga than in GGG. The mean crystal grain size (D) of the films was calculated from the broadening of the diffraction lines [(400), (420), (422), and their second orders] by using a Williamson Hall plot.[36] The size D slightly increases from 53 to 65 nm as the oxygen pressure decreases from 10 to 3 Pa. The kinetic energy of the ablated species increases as the oxygen pressure decreases because of the decrease in the number of collisions with ambient gas. Higher kinetic energy induces larger mobility of the clusters on the surface of the growing film, which explains why the growth of larger crystals can be promoted with the decrease in the ambient pressure.

As the oxygen pressure decreases to 1 Pa, whereas the films deposited on the YAG substrate are amorphous with [Ga]:[Gd] ~ 1, the films deposited on the YAP substrate have a strongly different crystalline structure. Figure 2(c) shows the XRD pattern of the film grown at $p_O = 1$ Pa on the YAP substrate; it consists of three narrow and strong diffraction peaks located at 23.22°, 47.36°, and 74.04° with corresponding d spacing equal to 3.828, 1.918, and 1.279 Å, respectively. With respect to the film composition, these peaks can be associated with the three orders of reflections from (002) planes of $GdGaO_3$ crystals (d equal to 3.8105, 1.905, and 1.27 Å, PDF 00-70-0238). The small displacement for larger d spacing, which is 0.68% for the (002) reflection, for example, is probably due to the presence of mechanical stress. All three orders of the reflections from (002) planes are strong with a very small broadening. The full separations due to $K\alpha_1$ and $K\alpha_2$ lines are clearly visible on the third order (006) reflection of the film, like for the (060) reflection of the YAP single crystal substrate, which indicates the high crystalline quality of the film.

In order to characterize the in-plane and out-of-plane orientation of the film relative to the substrate, rocking curves (ω-scan) for the (040) reflection of the substrate and the (004) reflection of the film (Fig. 3) were measured for different values of the φ azimuthal angle. According to these patterns, the normal to the (004) planes of the film is tilted by about 0.7° relative to the normal of the (010) planes of the substrate as a consequence of the lattice mismatch between the substrate and the growing film. The diffraction peak of the film is broader (FWHM = 0.32°) than that of the single crystal substrate (0.06°, which corresponds to the experimental setup resolution) indicating the presence of microstructural defects. To obtain a more detailed picture of the film growth, the pole figure of the (101) reflection was recorded (Fig. 4). Only two sharp peaks at $\chi = 55°$ with opposite azimuth $\phi = 0$ and 180° are observed and correspond to the (101) reflections related to a (001) growth direction. This figure proves the single crystalline and single domain growth relative to the substrate with a good coherence.

As already mentioned above, both $GdGaO_3$ (GGP) and YAP crystallize in orthorhombic structures and have the same crystal space group Pbnm(62). The growth regime, for which the (001) plane of the GGP film is parallel to the (010) YAP surface, can be

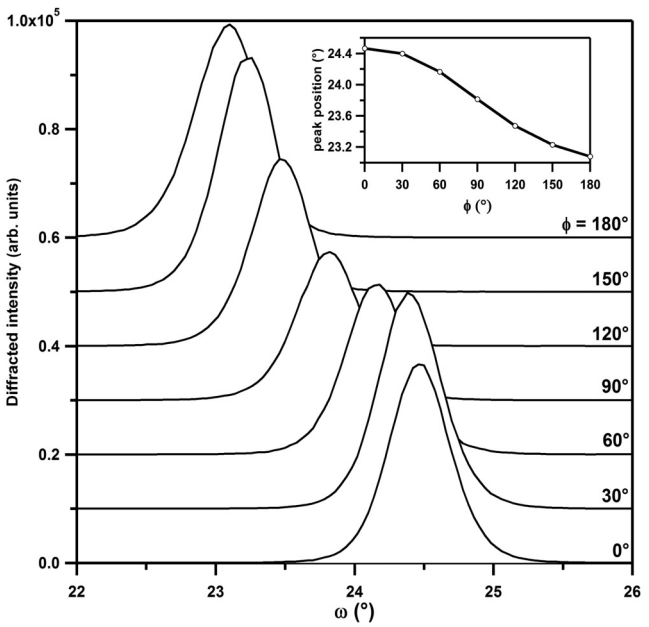


**FIG. 3.** ω-scans of (004) reflection at 2Θ = 47.64° for the GGP film deposited on the YAP substrate for different values of the azimuthal ϕ angle. The normal to the (010) plane of the substrate was aligned with the ϕ rotation axis. The curves are shifted vertically for the sake of clarity. The deviation of the ω peak position vs ϕ is reported in the inset figure.

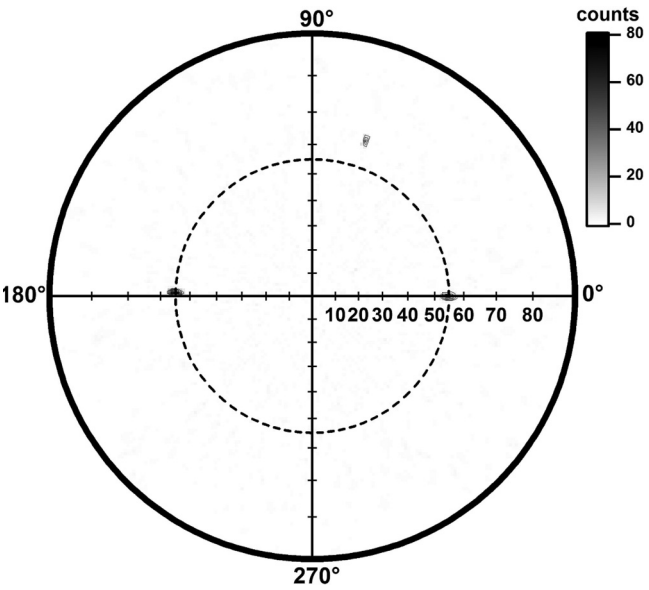


**FIG. 4.** Pole figure of the (001) reflection of the GGP film deposited on the YAP substrate. The dashed circle corresponds to χ = 55°.

simply explained by minimizing the lattice mismatch lm, [lm = ($d_{film}$ − $d_{substrate}$)/$d_{substrate}$)] between film and substrate. The YAP (010) surface has a quasi-square structure with a = 5.33 Å and c = 5.18 Å. The (001) plane of $GdGaO_3$ has also a nearly square structure with side a = 5.33 Å and b = 5.55 Å. Thus, in the case where the GGP (001) plane is parallel to the (010) plane of the YAP substrate, the lm is only 2.9% and 4.1%, if we take $a_{film}$ with $c_{substrate}$ and $b_{film}$ with $a_{substrate}$, respectively.

The effect of the laser energy density on the crystalline structure of the films was negligible at 2 and 4 J/cm$^2$. On the contrary, at low energy density, 0.5 J/cm$^2$, the XRD peaks associated with GGP become significantly broader and weaker and also peaks corresponding to the formation of GGG crystals appear. This could be explained by a decrease in the energy of the ablated species, which bombard the surface of the growing films. In this way, the growth conditions are closer to the equilibrium process. It was indeed presented that GGG crystallizes first and preferentially at temperatures lower than critical (around 1750 °C) from $Gd_2O_3$–$Ga_2O_3$ liquid at equilibrium conditions.[20] On the other hand, at a higher laser energy density (6 J/cm$^2$), the diffraction peaks become again much broader due to the creation of additional crystalline defects and the slight variation of the composition of films.

Figure 5 represents the XRD pattern of the film deposited in pure argon ambient. As follows from the RBS measurements, the deposited film was gallium free and the composition was that of gadolinium oxide when the oxygen gas was fully replaced by argon. Only two peaks at 28.44° and 47.44° in 2θ, beside the reflection from the YAP substrate, are present on the XRD pattern. Gadolinium oxide can exist in monoclinic or cubic phases so that it is questionable to determine the film crystalline structure using only this XRD pattern with two lines, which could be assigned to any of these structures. This ambiguity could be resolved through fluorescence experiments. The absence of the fluorescence emission from the $^3P_0$ level of $Pr^{3+}$ ions, which is characteristic of the cubic

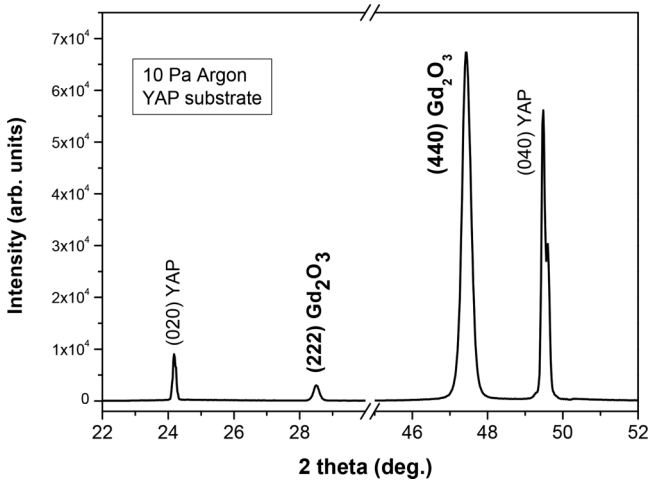


**FIG. 5.** XRD pattern of the film deposited on the YAP substrate at 10 Pa of argon.

sesquioxides, excludes any presence of the monoclinic phase (see below). Therefore, the XRD peaks can be associated with the reflections by the (222) and (440) crystalline planes of cubic $Gd_2O_3$ (PDF 00-43-1014). Taking into account the relative intensities of diffraction peaks from (111) and (110) planes, we conclude that the $Gd_2O_3$ film on the YAP substrate is strongly (110) textured, with a crystal size around 80 nm. This preferential orientation can be explained by minimizing the lattice mismatch. If the film $Gd_2O_3$ film grew with the (100) plane parallel to the surface, the lm would reach 1.4% and 4.3%, respectively, depending on the orientations. The (110) plane of $Gd_2O_3$ has a rectangular structure with sides equal to a = 10.81 Å and $a\sqrt{2} = 15.27$ Å, respectively. The lm of this rectangle relative to that with 2a and 3c of the YAP quasi-square (010) surface is equal to 1.4% and −1.7%, respectively. In the cubic sesquioxides phase, the denser planes are (111) ones; therefore, they have a lower surface free energy.[37] The minimization of the free surface energy could be the reason for the presence of a small peak at 28.44° associated with the reflection from the (111) plane of cubic $Gd_2O_3$.

### C. Fluorescence properties

The $Pr^{3+}$ fluorescence spectra were registered in the blue ($^3P_0 \rightarrow {}^3H_4$ transition) and in the orange-red ($^3P_0 \rightarrow {}^3H_6$, $^1D_2 \rightarrow {}^3H_4$, and $^3P_0 \rightarrow {}^3F_2$ transitions) regions for all films and compared to those of the crystalline phases mentioned above: garnet, perovskite, and sesquioxide. In GGG, $Pr^{3+}$ ions predominantly occupy the dodecahedral $Gd^{3+}$ sites with $D_2$ symmetry. In this position, all optical transitions from $^3P_{0,1,2}$ and $^1D_2$ levels are allowed. More details about the spectroscopic properties of this crystal can be found in Ref. 38. The fluorescence properties of Pr:$GdGaO_3$ have not been presented so far, but are expected to be similar to those of the isomorphous Pr: YAP crystal. In orthorhombic YAP, the $Pr^{3+}$ ion enters the lattice at yttrium sites having $C_S$ point symmetry. For ions in this symmetry, all optical transitions are allowed.[26] Because of the strong crystal anisotropy, the absorption and emission spectra depend strongly on the crystal orientation. The details of Pr:YAP fluorescence properties can be found in several publications, such as Refs. 26 and 39. In cubic sesquioxide, the $Pr^{3+}$ ions occupy two different cation sites with site symmetry $C_2$ and $S_6$. The $^3P_0$ emission is absent in the emission spectra of both sites $C_2$ and $S_6$, and only the transitions from $^1D_2$ were observed.[40] On the contrary, in monoclinic $Gd_2O_3$ doped with Pr, strong emission lines issued from $^3P_{0,1,2}$ levels were observed.[41] Significantly different spectra were obtained for different kinds of films and, because of the sensitivity of the $Pr^{3+}$ ions to the site symmetry, helped to confirm or refine their crystalline structure.

Figure 6 shows the evolution of the fluorescence spectra associated with the $^3P_0 \rightarrow {}^3H_4$ transition of $Pr^{3+}$ ions, when the crystalline structure of the film is changed from the GGG oriented film to the amorphous one. The excitation was into the $^3P_2$ multiplet at 450 nm. The fluorescence of the well crystalline and oriented Pr:GGG films shown in Fig. 6(a) (deposited on the YAG substrate at $p_O$ = 5 Pa) is very close to the single crystal one (dashed line). The strongest lines at 485.5 and 486.5 nm correspond to transitions from $^3P_0$ to the lowest sublevels $\Gamma_3$ and $\Gamma_4$ of the $^3H_4$ ground multiplet and are clearly separated. On the contrary, for the YAP

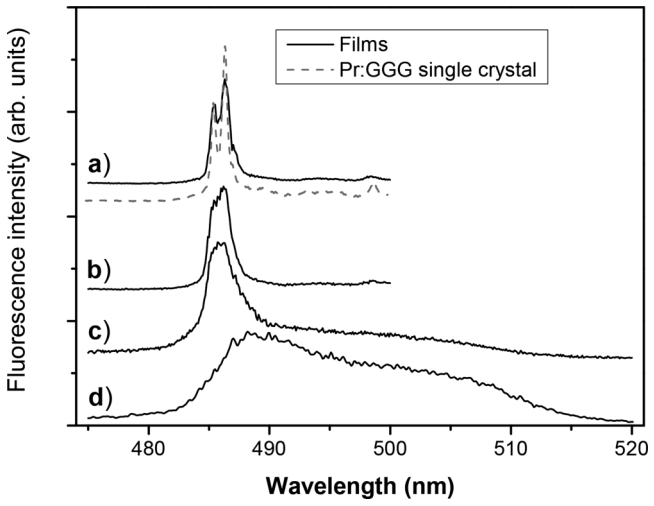


**FIG. 6.** $^3P_0 \rightarrow {}^3H_4$ fluorescence spectra of films deposited (a) on YAG $p_O$ = 5 Pa-(100) orientated GGG, (b) on YAP $p_O$ = 5 Pa-polycrystalline GGG, (c) on YAG $p_O$ = 3 Pa (100) orientated GGG, and (d) YAG $p_O$ = 1 Pa-amorphous film, respectively ($\lambda_{exc}$ = 450 nm).

substrate [Fig. 6(b)] and identical deposition conditions, these lines are not separated and the spectrum consists of an unresolved broad peak centered at 486 nm. This has to be the consequence of the nanosize and polycrystalline character of the film and the presence of many perturbed sites at the crystal grain boundaries. When the film is deposited on the YAG substrate at the lower oxygen pressure of 3 Pa, it becomes Ga deficient, consists of GGG crystals embedded in an amorphous phase [Fig. 6(c)], and the 486 nm line is superimposed over broad bands located at 490 and 500 nm. These bands may be attributed to the fluorescence of $Pr^{3+}$ in this amorphous phase, by comparison with the spectrum of the fully amorphous film of the same composition, which was grown at $p_O$ = 1 Pa on YAG [Fig. 6(d)]. The peak at 486 nm disappears and only the broad bands at 490 and 500 nm, characteristic of the fluorescence of $Pr^{3+}$ in amorphous materials, are observed as was already described in Refs. 18 and 38.

The fluorescence spectrum of the Pr:$GdGaO_3$ film deposited on the YAP substrate, registered in the blue range under excitation to the $^3P_2$ level at 447 nm, is plotted in Fig. 7. The fluorescence in the range 470–486 nm is associated with the transitions between $^3P_1$+$^1I_6$ and the $^3H_4$ ground multiplet, whereas the 489–510 nm range corresponds to $^3P_0$ to $^3H_4$ transitions. For comparison, the spectra of a Pr:YAP crystal are presented for three different excitation/emission geometries relative to the three crystal axes: the excitation $\mathbf{k_{exc}}$ vector was respectively parallel to a, b, and c axes (see the description of YAP crystal in Sec. II) whereas the emission $\mathbf{k_{em}}$ vector, perpendicular to $\mathbf{k_{exc}}$, was respectively parallel to the c and a axes. Even if the emission spectra were registered without any polarization direction selection, so that no precise symmetry could be assigned to each transition, these three spectra clearly give the positions of all different transitions, in agreement with Ref. 26, and emphasize that their relative intensities depend on the geometry.

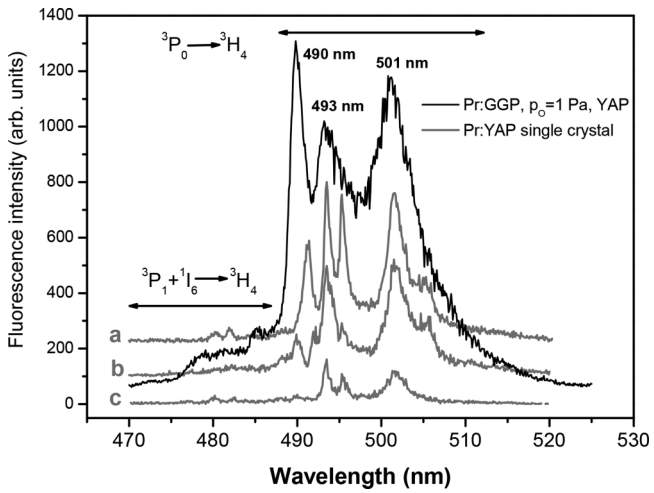


**FIG. 7.** $^3P_0 \rightarrow {}^3H_4$ fluorescence spectrum of GGP films deposited on the YAP substrate at $p_O = 1$ Pa ($\lambda_{exc} = 447$ nm).

The film spectrum is composed of three broad peaks, positioned at 490, 493, and 501 nm, which may be attributed to the transitions from $^3P_0$ to some of the different Stark sublevels of the $^3H_4$ ground state. Although all different transitions cannot be resolved for GGP, the spectrum profile and the positions of the lines agree with the energies of the YAP sublevels reported in Ref. 26.

Figure 8 shows the fluorescence spectra in the spectral range 590–680 nm of the Pr:GGG, Pr:$GdGaO_3$, and Pr:$Gd_2O_3$ crystalline films deposited at $p_O = 5$ Pa on YAG [Fig. 8(a)], $p_O = 1$ Pa on YAP [Fig. 8(b)], and $p_{Ar} = 10$ Pa on YAP [Fig. 8(c)], respectively. In this wavelength zone, emissions from both $^3P_0$ and $^1D_2$ levels are observed. As can be seen, the spectrum of each of these films is different and either agrees well with the fluorescence of cubic Pr:GGG or cubic Pr:$Gd_2O_3$ (Ref. 40) crystals, included in the figure for comparison, or is very similar to the fluorescence spectrum of orthorhombic Pr:YAP.[26]

The fluorescence decays from $^3P_0$ for Pr:GGG and Pr:$GdGaO_3$ and from $^1D_2$ in the case of Pr:$Gd_2O_3$ were measured and show significant differences in agreement with the lifetime values expected for these different materials. All fluorescence decays were almost exponential. The measured values of the $^3P_0$ and $^1D_2$ lifetimes are summarized in Table I. For Pr:GGG films, there is a good agreement with the bulk crystal value.[18] For the Pr:GGP film, the 11 $\mu$s value of the $^3P_0$ decay time is very similar to the 10 $\mu$s one reported for Pr:YAP crystal.[26] For the Pr:$Gd_2O_3$ film, the $^1D_2$ decay time of 57 $\mu$s is significantly shorter than the value reported in Ref. 41 for a 0.1% doped $Gd_2O_3$ crystal, which could be due to the higher concentration of praseodymium in the films.

### D. Optical properties

The refractive indices of the films are summarized in Table I. For each film, a good agreement was found between the thicknesses determined at the two different wavelengths and two polarizations,

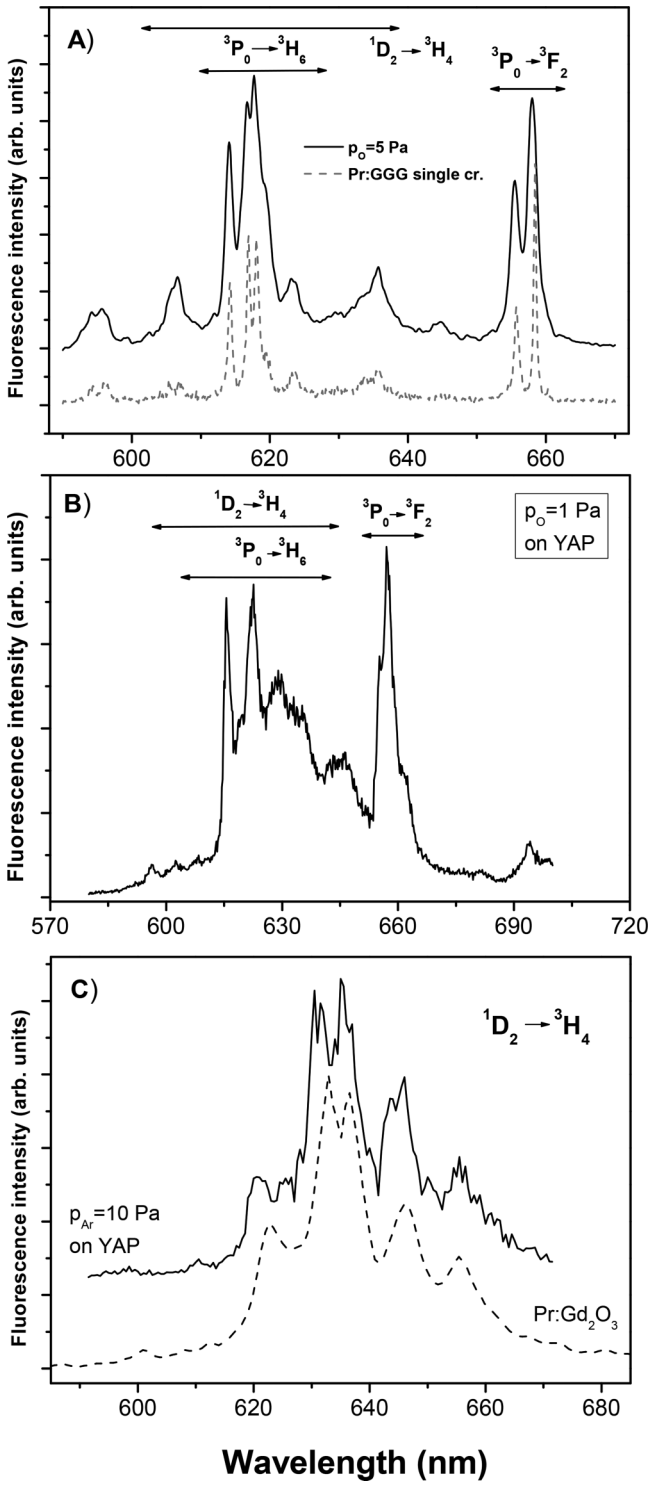


**FIG. 8.** Fluorescence spectra of (a) Pr:GGG, (b) Pr:GGP, and (c) Pr:$Gd_2O_3$ films. The dashed line corresponds to the spectra of Pr:GGG single crystal and Pr:$Gd_2O_3$ powder (Ref. 41).

which confirms that the step index profile model used for calculation is appropriate.[42]

The refractive indices of oriented crystalline GGG films deposited at $p_O = 5–10$ Pa on YAG were determined to be $n_{TE} = 1.96$ and $n_{TM} = 1.964$ at 632.8 nm with accuracy in the range of ±0.001, close to the value of 1.965 measured for the Pr:GGG single crystal target.[18] Apart from the $GdGaO_3$ film deposited at 1 Pa on the YAP substrate, which is discussed below, the films grown at decreasing ambient oxygen pressure have an increasing refractive index due to increasing gallium deficiency. For the textured Pr:$Gd_2O_3$ film, a value of $n_{TE} = 1.977$ at 632.8 nm was measured, which is in reasonable agreement with the refractive index of undoped cubic $Gd_2O_3$, equal to $1.979 \pm 0.001$ at 589.3 nm, taking into account that the refractive index may be slightly modified by Pr doping.[43] The differences between the $n_{TE}$ and $n_{TM}$ refractive indices of all these films are of the same order of magnitude as the measurement accuracy, which indicates that the films are isotropic, in agreement with either their cubic crystalline phase (GGG or $Gd_2O_3$) or their amorphous structures.

Because no data about the refractive index of $GdGaO_3$ were found in the literature, special attention was paid to its determination. As the orthorhombic cell is anisotropic and the film grows exclusively with (001) orientation, the film shows strongly anisotropic refractive indices and $n_{TE} = 2.0714$ and $n_{TM} = 2.0275$ with an accuracy of ±0.0002 were measured at 632.8 nm wavelength.

Waveguiding propagation was not observed for the polycrystalline GGG and textured $Gd_2O_3$ films deposited on the YAP substrate, probably because of the high scattering induced by the crystalline grains. On the other hand, the oriented GGG and amorphous Ga deficient GGG films deposited on the YAG substrate show a nice waveguiding effect with a bright outcoupled spot at the end of the waveguides. Because of the small size of the films, however, it was not possible to accurately analyze the exponential decay of the scattered light recorded with a CCD camera along the propagation line. Concerning this measurement, however, a low attenuation (≤1 dB/cm) can be suggested. The propagation line was observed also for the Pr:$GdGaO_3$ film, and the waveguiding attenuation in the range of 2.2–2.5 dB/cm can be estimated from a series of measurements performed at different places of the film. Such a value is still very promising for practical applications.

## IV. SUMMARY AND CONCLUSIONS

Three different compounds cubic $Gd_2O_3$, orthorhombic $GdGaO_3$, and cubic $Gd_3Ga_5O_{12}$ doped with $Pr^{3+}$ ions were fabricated as waveguiding films by pulsed laser deposition from the same target material: $Pr^{3+}$ doped $Gd_3Ga_5O_{12}$ (Pr:GGG) single crystal. All of them were deposited at the same substrate temperature, 800 °C, and the different crystalline phases were obtained by only changing the ambient oxygen pressure and the substrate type [(100) YAG or (110) YAP single crystals].

At oxygen pressures in the range 5–10 Pa, (100) oriented or polycrystalline Pr:GGG films were obtained on YAG and YAP substrates, respectively. At an oxygen pressure equal to 1 Pa, orthorhombic Pr:$GdGaO_3$, epitaxially grown along a (001) direction, was deposited on (010) YAP substrates, whereas amorphous Ga deficient films were obtained on the YAG substrate. At 10 Pa of argon ambient atmosphere, a textured cubic Pr:$Gd_2O_3$ film was deposited on the YAP substrate. The Ga loss of the single crystal Pr-doped GGG target induced by the KrF laser was the reason for the strong dependence of the composition of the deposited films on the partial oxygen pressure during the laser ablation process.

$Pr^{3+}$ fluorescence properties of the films of various composition were found similar to those of the corresponding bulk crystals, without any parasitic phase, thus confirming the XRD phase identification and the correct conservation of the Pr ions doping rate. Moreover, the fluorescence spectrum of the Pr:$Gd_20_3$ film, showing only the emission from the $^1D_2$ multiplet, allows us to exclude any monoclinic structure for this film.

The refractive indices of the films agree with those of bulk crystals. The oriented crystalline Pr:GGG films show waveguided propagation with an attenuation lower than 1 dB/cm.

Gadolinium orthogallate ($GdGaO_3$) thin film was successfully epitaxially grown on the YAP substrate. We determined the fluorescence properties of the $Pr^{3+}$ doping ions and the refractive indices, which have not been reported up to now. The fluorescence spectra of the Pr-doped GGP film were found to be similar to the fluorescence of Pr:YAP crystal, with a $^3P_0$ lifetime of 11 $\mu$s. The refractive indices of Pr:GGP are higher than those of YAP crystal ($n = 1.916$ at 632.8 nm) and equal to $n_{TE} = 2.0714$ and $n_{TM} = 2.0275$ at 632.8 nm wavelength. The Pr:GGP film shows waveguided propagation with an attenuation around 2.5 dB/cm, which is promising for application as a planar waveguide. Concerning applications in the field of scintillators, the higher density of this crystal relative to the commonly used isomorphous YAP crystal should be considered very favorable.

## ACKNOWLEDGMENTS

This work was supported by the Science Foundation (Project No. 18-17834S) and the Ministry of Education, Youth and Sports (Project No. SOLID21 CZ.02.1.01/0.0/0.0/16_019/0000760).

## DATA AVAILABILITY

The data that support the findings of this study are available from the corresponding author upon reasonable request.

## REFERENCES

[1]D. B. Chrisey and G. K. Hubler, *Pulsed Laser Deposition of Thin Films* (Wiley, New York, 1994).
[2]R. W. Eason, S. J. Barrington, C. Grivas, T. C. May-Smith, and D. P. Shepherd, *Pulsed Laser Deposition of Thin Films* (John Wiley & Sons, Inc., Hoboken, NJ, 2006), pp. 383–420.
[3]J. A. Grant-Jacob, S. J. Beecher, J. J. Prentice, D. P. Shepherd, J. I. Mackenzie, and R. W. Eason, Surf. Coat. Technol. **343**, 7 (2018).
[4]V. Nazabal *et al.*, Thin Solid Films **518**, 4941 (2010).
[5]J. Huang *et al.*, Adv. Opt. Mater. **6**, 1800510 (2018).
[6]H. M. Ju, X. B. Feng, T. H. Song, W. C. Liu, C. L. Mak, and W. Huang, J. Alloys Compd. **749**, 967 (2018).
[7]A. Pillonnet, J. Lancok, C. Martinet, O. Marty, J. Bellessa, and C. Garapon, J. Phys.: Condens. Matter **18**, 10043 (2006).
[8]J. Schou, Appl. Surf. Sci. **255**, 5191 (2009).
[9]C. N. Bell, D.-C. Lee, M. N. Drexler, C. M. Rouleau, K. Sasaki, S. D. Senanayake, M. D. Williams, and F. M. Alamgir, Thin Solid Films **717**, 138437 (2021).

[10]D. Luca, J. Optoelectron. Adv. Mater. **7**, 625 (2005).
[11]M. B. Korzenski, P. Lecoeur, B. Mercey, D. Chippaux, B. Raveau, and R. Desfeux, Chem. Mater. **12**, 3139 (2000).
[12]D. Tenciu *et al.*, Dig. J. Nanomater. Bios. **7**, 393 (2012).
[13]J. A. G. de León, A. Pérez-Centeno, G. Gómez-Rosas, E. Camps, J. S. Arias-Cerón, M. A. Santana-Aranda, and J. G. Quiñones-Galvan, Mater. Res. Express **7**, 016423 (2020).
[14]M. Novotný *et al.*, J. Phys. D: Appl. Phys. **45**, 225101 (2012).
[15]H. von Wenckstern, D. Splith, and M. Grundmann, in *Gallium Oxide: Materials Properties, Crystal Growth, and Devices*, edited by M. Higashiwaki and S. Fujita (Springer International, Cham, 2020), pp. 273–291.
[16]A. Perrone, Jpn. J. Appl. Phys. **41**, 2163 (2002).
[17]P. A. Atanasov, M. Jiménez de Castro, A. Perea, J. Perrière, J. Gonzalo, and C. N. Afonso, Appl. Surf. Sci. **186**, 469 (2002).
[18]J. Lancok, C. Garapon, M. Jelinek, J. Mugnier, and R. Brenier, Appl. Phys. A **81**, 1477 (2005).
[19]M. A. DiGiuseppe, S. L. Soled, W. M. Wenner, and J. E. Macur, J. Cryst. Growth **49**, 746 (1980).
[20]J. Nicolas, J. Coutures, J. P. Coutures, and B. Boudot, J. Solid State Chem. **52**, 101 (1984).
[21]J. R. Carruthers, M. Kokta, R. L. Barns, and M. Grasso, J. Cryst. Growth **19**, 204 (1973).
[22]Y. Sharma, S. P. Pavunny, J. F. Scott, and R. S. Katiyar, ECS Trans. **66**, 287 (2015).
[23]M. Marezio, J. P. Remeika, and P. D. Dernier, Inorg. Chem. **7**, 1337 (2002).
[24]S. Geller, P. J. Curlander, and G. F. Ruse, Mater. Res. Bull. **9**, 637 (1974).
[25]J. C. Guitel, M. Marezio, and J. Mareschal, Mater. Res. Bull. **11**, 739 (1976).
[26]M. Malinowski, C. Garapon, M. F. Joubert, and B. Jacquier, J. Phys.: Condens. Matter **7**, 199 (1995).
[27]P. Pues, M. Laube, S. Fischer, F. Schröder, S. Schwung, D. Rytz, T. Fiehler, U. Wittrock, and T. Jüstel, J. Lumin. **234**, 117987 (2021).
[28]D. Hreniak, M. Bettinelli, A. Speghini, A. Łukowiak, P. Głuchowski, and R. Wiglusz, J. Nanosci. Nanotechnol. **9**, 6315 (2009).
[29]T. J. de Prinse *et al.*, Adv. Opt. Mater. **9**, 2001903 (2021).
[30]J. Lancok, M. Novotný, C. Garapon, and M. Jelínek, J. Phys.: Conf. Ser. **59**, 400 (2007).
[31]S. Chénais, F. Druon, F. Balembois, P. Georges, A. Brenier, and G. Boulon, Opt. Mater. **22**, 99 (2003).
[32]L. Ortega, C. Bouchard, R. Bruyère, and P. Bordet, J. Phys. IV **118**, 71 (2004).
[33]R. Ulrich and R. Torge, Appl. Opt. **12**, 2901 (1973).
[34]M. D. Himel and U. J. Gibson, Appl. Opt. **25**, 4413 (1986).
[35]C. D. Brandle, V. J. Fratello, A. J. Valentino, and S. E. Stokowski, J. Cryst. Growth **85**, 223 (1987).
[36]H. P. Klug and L. E. Alexander, *X-ray Diffraction Procedures for Polycrystalline and Amorphous Materials* (John Wiley & Sons, New York, 1974).
[37]O. Pons-Y-Moll, J. Perriere, E. Millon, R. M. Defourneau, D. Defourneau, B. Vincent, A. Essahlaoui, A. Boudrioua, and W. Seiler, J. Appl. Phys. **92**, 4885 (2002).
[38]A. Lupei, H. Gross, and P. Reiche, J. Phys.: Condens. Matter **7**, 5701 (1995).
[39]A. A. Kaminskii, *Crystalline Lasers* (CRC, Boca Raton, FL, 2020).
[40]G. C. Aumüller, W. Köstler, B. C. Grabmaier, and R. Frey, J. Phys. Chem. Solids **55**, 767 (1994).
[41]M. Arai, N. Matsuda, and M. Tamatani, J. Alloys Compd. **192**, 45 (1993).
[42]Y.-C. Wu, M. Villanueva-Ibañez, C. Le Luyer, J. Shen, and J. Mugnier, Proc. SPIE **5946**, 59461E (2006).
[43]O. Medenbach, D. Dettmar, R. D. Shannon, R. X. Fischer, and W. M. Yen, J. Opt. A: Pure Appl. Opt. **3**, 174 (2001).